PROBING OF A BOILING LAYER WITH LASER RADIATION

Yu. A. Popov, V. M. Kalemenev,
B. P. Kartashov, and R. V. Khomyakov

UDC 66.096.5

The distribution function over optical depth, correlation function, and effective optical depth are experimentally determined in the bed space of a boiling layer. Results are compared with calculations based on model concepts of the boiling layer.

A boiling layer is divided into two regions: a region of constant density and one of rapidly decreasing material density. The latter region is sometimes termed the bed space. The goal of the present study is a clarification of the structure of this bed space.

1. A fluidized layer was created in a vertical reactor with square section 100 × 100 mm. The layer was fluidized by air. The air enters the reactor from the bottom through a funnel covered by two wire grids between which a woven fabric is located. The grids are attached to the mesh body. The chamber walls through which radiation was passed are prepared of window glass. The beam of an LG 126 laser was expanded by a diverging lens and shaped with a slit. Adjustment was performed at a wavelength $\lambda = 0.63$ μ, and measurements at $\lambda = 0.63$, 1.15, 3.36 μ. The beam area in the reactor was 96 mm^2. After exiting from the vessel the beam was focussed by a lens on an FD-3 photodiode, connected to an N-700 oscilloscope. Tests revealed that over the range of measurements the photocurrent is proportional to the radiant energy flux incident on the photodiode. A schematic diagram of the apparatus is shown in Fig. 1. The detector capture angle for radiation scattered by particles was about 1/300. Over equal time intervals ($\Delta t_i = 0.02$ sec) the value I/I_0 was found. From the relationship

$$I_i/I_0 = e^{-\tau_i} \tag{1}$$

instantaneous values of optical thickness were calculated and histograms of density distribution over τ were constructed. The mean value of τ

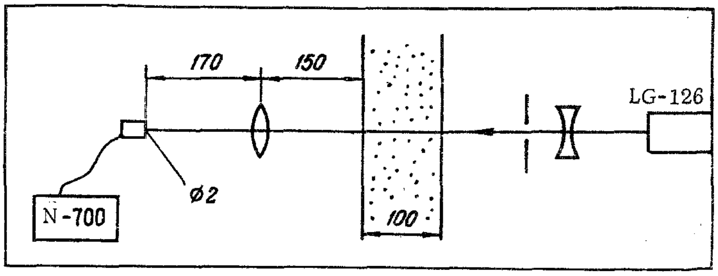

Fig. 1. Optical diagram of apparatus.

All-Union Scientific-Research Institute of Metallurgical Thermophysics, Sverdlovsk.
Translated from Inzhenerno-Fizicheskii Zhurnal, Vo. 28, No. 3, pp. 465-471, March, 1975. Original article submitted May 25, 1974.

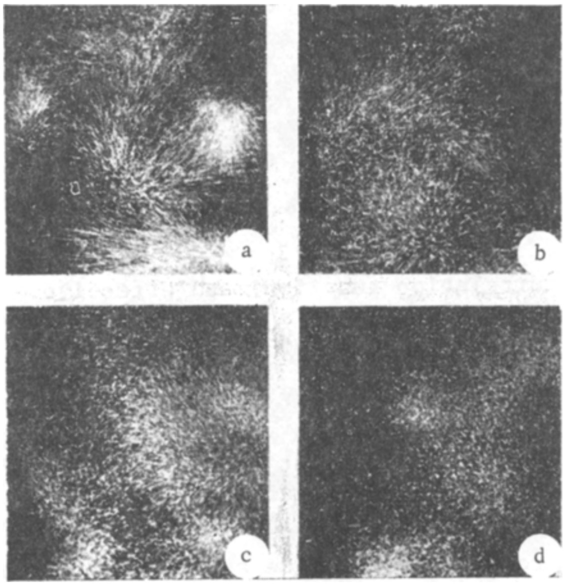

Fig. 2. Photos of fluidized layer obtained in 100 × 100 mm chamber by photography from above. Layer illuminated by an arc light source. Light beam formed to irradiate chamber layer at height h above bottom. Light beam thickness 20 mm, width 100 mm: a) h = 129 mm, exposure 1/25 sec; b) 129 and 1/50; c) 129 and 1/100; d) 129 and 1/250.

$$\langle \tau \rangle = \frac{1}{N} \sum_{i=1}^{N} \tau_i, \tag{2}$$

the correlation function [2]

$$K_\tau (n\Delta t_1) = \frac{1}{N-n} \sum_{i=1}^{N-n} \tau_i \tau_{i+n} - \langle \tau \rangle^2 \tag{3}$$

and effective optical thickness

$$\tau_{ef} = -\ln\left[\frac{1}{N} \sum_{i=1}^{N} I_i/I_0\right]. \tag{4}$$

were determined. Approximately N ≃ 300 samples were used. I_i values were taken from the oscilloscope screen manually and processed by a Minsk-25 computer.

Two series of experiments were performed. The first series used river sand with mean particle diameter d = 0.45 mm and particle size distribution dispersion σ_d^2 = 0.0085 mm^2. Air velocity in the chamber (measured by expenditure) was 1.4 m/sec. Mass of the charge was 630 g.

The second series of experiments used corundum particles 60 μ in diameter with an air velocity of 0.33 m/sec. The corundum mass in the chamber was 125 g.

The particle distribution in the chamber in the first case was extremely nonuniform. On the average, several clusters of material were located in the beam path (Fig. 2).

2. Considering the extremely nonuniform distribution of material in the boiling layer (Fig. 1) we will assume the validity of the packet model. We note that the particle concentration in a packet is lower than the concentration in the filled layer and that the packet does not have sharply defined boundaries (Fig. 2). We assume that the probability of finding n packets along the light path is determined by the Poisson formula [1] and that the optical path of a ray in the packet may vary.

Comparison with experiment indicates that the density distribution of optical paths for one packet may be given in the form of the gamma distribution

$$\varphi(\tau) = \frac{\alpha^{m+1}}{\Gamma(m+1)} \tau^m e^{-\alpha\tau}. \tag{5}$$

The mean optical thickness τ_1 of the packet is connected with the parameter α by the function

$$\tau_1 = \frac{m+1}{\alpha}. \tag{6}$$

The density distribution over optical thicknesses for the layer will have the form [3]

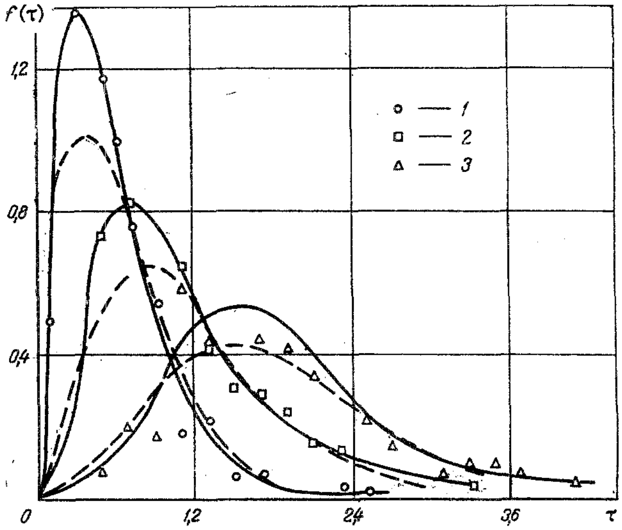

Fig. 3

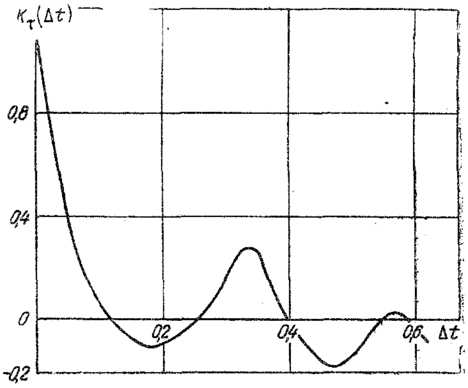

Fig. 4

Fig. 3. Density distribution over optical thicknesses (dashed, calculation; solid curves, from histograms): 1) h = 133 mm; 2) 123 mm; 3) 109 mm.

Fig. 4. Correlation function (h = 109 mm). Δt, sec.

$$f(\tau) = e^{-\bar{n}}\,\delta(\tau) + xe^{-\bar{n}-\alpha\tau} \sum_{n=1}^{\infty} \frac{x^{(m+1)\,n-1}}{n!\,\Gamma[(m+1)\,n]}, \tag{7}$$

where $x = \alpha\bar{n}^{1/(m+1)}$.

For the mean value and dispersion from Eq. (7) we find

$$\langle \tau \rangle = \bar{n}\tau_1, \tag{8}$$

$$\sigma^2 = K_\tau(0) = \frac{4}{3}\langle \tau \rangle \tau_1. \tag{9}$$

For the mean value of the transmission from Eq. (7) we obtain

$$\langle e^{-\tau} \rangle = \exp\left\{-\bar{n}\left[1-\left(\frac{\alpha}{1+\alpha}\right)^{m+1}\right]\right\}, \tag{10}$$

i.e.,

$$\tau_{\text{эф}} = \bar{n}\left[1-\left(\frac{\alpha}{1+\alpha}\right)^{m+1}\right]. \tag{11}$$

The parameter m is the drive parameter. Analysis of experimental results shows that the value m = 2 fits the data satisfactorily. Table 1 shows a calculation of the function

$$F(x) = e^{-x/2} \sum_{n=1}^{\infty} \frac{x^{3n-1}}{n!\,(3n-1)!}. \tag{12}$$

The density Eq. (7) is easily expressed in terms of Eq. (12).

TABLE 1

x	$F(x)$	x	$F(x)$	x	$F(x)$
0	0	12	9,4031	55	51,755
1	0,3058	14	12,634	60	43,944
2	0,7852	16	16,356	65	35,616
3	1,2361	18	20,505	70	27,784
4	1,6974	20	24,985	75	20,846
5	2,2234	25	36,852	80	15,109
6	2,8742	30	47,933	85	10,606
7	3,6384	40	61,083	90	7,226
8	4,5291	43	61,785	95	4,789
9	5,5488	45	61,426	100	3,092
10	6,7000	50	57,983		

TABLE 2

h, mm	$\bar{n}$	τ_1	$\langle\tau\rangle$	τ_{ef}	τ_{ef}, calc
133	2,6	0,23	0,595	0,524	0,525
123	4,1	0,27	1,12	0,944	0,945
113	5,2	0,305	1,59	1,37	1,30
109	5,1	0,38	2,01	1,64	1,61
105	4,6	0,59	2,70	1,95	1,96

3. Figure 3 depicts a comparison of experimental and theoretical results for density distribution over optical thickness of the layer for the first series of experiments.

Table 2 offers a summary of experimental results for various probe heights in a boiling layer of river sand.

The $\bar{n}$ data of Table 2 were obtained from Eqs. (8), (9) for experimental values of $\langle\tau\rangle$ and σ^2. The last column of Table 2 presents results of calculating τ_{ef} from Eq. (11).

Figure 4 shows the correlation function for river sand at h = 109 mm. In all calculations m was taken as 2. This produces the best agreement with experiment.

Results of the first series of experiments were independent of radiation wavelength. The particle size parameter $\rho = \pi d/\lambda$ is greater than 300. A portion of the radiation scattered by particles due to Fraunhoffer diffraction is centered in a narrow cone with angle $\alpha_0 \sim 1/\rho$ [5]. Thus, practically all the diffracted radiation fell on the detector. The dimensionless coefficient of attenuation for coarse particles is equal to two, and the dimensionless coefficient of distance produced by Fraunhofer diffraction is equal to unity. It thus follows that the attenuation section for the first series of experiments may be taken equal to the transverse particle section, as follows from geometric optics. From this we obtain a simple relationship between the mean optical thickness and the mean particle weight concentration C (g/cm^3)

$$\langle\tau\rangle = \frac{3}{2}\cdot\frac{lC}{\rho d}, \tag{13}$$

where ρ is the particle material's density and l is the thickness of the layer. In our case $\langle\tau\rangle$ = 126 C (g/cm^3).

It follows from the experimental results that the concentration decreases exponentially with layer height

$$C = C_0 e^{-\beta h}, \tag{14}$$

TABLE 3

h, mm	$\langle\tau\rangle$	σ^2
104	0,166	0,027
87	0,511	0,035
72	0,993	0,065

where $\beta = 0.5\ cm^{-1}$, $C_0 = 3.9\ g/cm^3$. The concentration cannot be greater than the bulk particle concentration, since Eq. (14) is invalid for small h. As is well known, for small h concentration is practically independent of h. If we assume that at h less than h_0 the concentration is constant and equal to the bulk concentration, then from Eq. (14) we obtain $h_0 \doteq 2$ cm. Now, with use of Eq. (14), it is simple to calculate the total mass of the charge, which was found to be 600 g, close to the actual value.

The proposal of exponential dependence of concentration in a boiling layer was first proposed in [6] and verified in [7]. Our study supports the exponential character of decrease in boiling layer concentration with height, beginning at some value h_0.

It is evident from Table 2 that the quantity $e^{-\langle\tau\rangle}$ for a boiling layer may differ significantly from the value of the mean transmission $\langle e^{-\tau} \rangle$. The form of the correlation function (Fig. 4) indicates the existence of the well known [4] boiling layer auto-oscillation.

For fine corundum particles, it follows from the experiment that $\langle e^{-\tau} \rangle \simeq e^{-\langle\tau\rangle}$ and the density $f(\tau)$ is close to Gaussian. The medium in this case is close to a pneumotransport state and quite homogeneous. Results of measurements at $\lambda = 1.15\ \mu$ are shown in Table 3.

The concentration in the second series of experiments may only be roughly estimated from Eq. (13). More accurate calculations should be performed with the Mie theory.

NOMENCLATURE

λ, Radiation wavelength; Δt_1, time interval; I, intensity of radiation through layer; I_0, intensity of radiation without layer; τ, optical thickness; K, correlation function; τ_{ef}, effective optical thickness; d, mean particle diameter; σ^2, dispersion; Γ, gamma function; $\bar{n}$, mean number of packets in light path; $f(\tau)$, density distribution over optical thickness for layer; τ_1, mean optical thickness of packet; $\langle\tau\rangle$, mean optical thickness of layer; l, layer thickness; C, mean particle concentration by weight in layer.

LITERATURE CITED

1. B. V. Gnedenko, A Course in Probability Theory [in Russian], Nauka (1965).
2. A. A. Sveshnikov, Applied Methods in the Theory of Random Functions [in Russian], Nauka (1968).
3. Yu. A. Popov, Inzh. Fiz. Zh., 25, No. 5, 842 (1973).
4. M. É. Aerov and O. M. Todes, Hydraulic and Thermal Principles in Operation of Apparatus with Stationary and Boiling Grain Layers [in Russian], Khimiya (1968).
5. G. Van de Hulst, Light Scattering by Small Particles [Russian translation], Inostr. Lit. (1961).
6. N. I. Syromyatnikov, Tr. Ural. Politekh. Inst., No. 41, Sverdlovsk (1955).
7. N. I. Syromyatnikov, L. K. Vasanov, R. D. Valulin, and A. I. Karpenko, Inzh. Fiz. Zh., 12, No. 5, 783 (1972).